

UC Irvine

UC Irvine Previously Published Works

Title

In vivo electrochemical lipolysis of fat in a Yucatan pig model: A proof of concept study

Permalink

<https://escholarship.org/uc/item/3642r6g0>

Journal

Lasers in Surgery and Medicine, 55(1)

ISSN

0196-8092

Authors

Park, Asher C
Chan, Carmen K
Hutchison, Dana M
et al.

Publication Date

2023

DOI

10.1002/lsm.23620




Copyright Information

This work is made available under the terms of a Creative Commons Attribution License, available at <https://creativecommons.org/licenses/by/4.0/>

Peer reviewed

PRECLINICAL REPORTS

In vivo electrochemical lipolysis of fat in a Yucatan pig model: A proof of concept study

Asher C. Park BS¹  | Carmen K. Chan MD² | Dana M. Hutchison MD, MSc¹ |
Urja Patel BS¹ | Ellen M. Hong BA³  | Earl Steward BS⁴ | Katelyn K. Dilley BS¹ |
Naya L. Sterritt⁵ | Sehwan Kim PhD⁶ | Michael G. Hill PhD⁷ | Joon S. You PhD⁸ |
Brian J. F. Wong MD, PhD^{1,2,5} 

¹Beckman Laser Institute & Medical Clinic, University of California–Irvine, Irvine, California, USA

²Department of Otolaryngology—Head and Neck Surgery, School of Medicine, University of California–Irvine, Orange, California, USA

³School of Medicine, Hackensack Meridian, Nutley, New Jersey, USA

⁴Department of Surgery, School of Medicine, University of California–Irvine, Orange, California, USA

⁵Department of Biomedical Engineering, University of California–Irvine, Irvine, California, USA

⁶Department of Biomedical Engineering, Beckman Laser Institute, Korea, Dankook University, Cheonan-si, Chungnam, Republic of Korea

⁷Department of Chemistry, Occidental College, Los Angeles, California, USA

⁸eLysis Inc., Laguna Niguel, California, USA

Correspondence

Brian J. F. Wong, MD, PhD, Beckman Laser Institute, University of California – Irvine, 1002 Health Sciences Rd, Irvine, CA 92697, USA.
Email: bjwong@uci.edu

Funding information

Ministry of Science and ICT,
Grant/Award Number: NRF-2018K1A4A3A02060572

Abstract

Objectives: Traditional fat contouring is now regularly performed using numerous office-based less invasive techniques. However, some limitations of these minimally invasive techniques include high cost or limited selectivity with performing localized contouring and reduction of fat. These shortcomings may potentially be addressed by electrochemical lipolysis (ECLL), a novel approach that involves the insertion of electrodes into tissue followed by application of a direct current (DC) electrical potential. This results in the hydrolysis of tissue water creating active species that lead to fat necrosis and apoptosis. ECLL can be accomplished using a simple voltage-driven system (V-ECLL) or a potential-driven feedback cell (P-ECLL) both leading to water electrolysis and the creation of acid and base in situ. The aim of this study is to determine the long-lasting effects of targeted ECLL in a Yucatan pig model.

Methods: A 5-year-old Yucatan pig was treated with both V-ECLL and P-ECLL in the subcutaneous fat layer using 80:20 platinum:iridium needle electrodes along an 8 cm length. Dosimetry parameters included 5 V V-ECLL for 5, 10, and 20 minutes, and –1.5 V P-ECLL, –2.5 V P-ECLL, –3.5 V P-ECLL for 5 minutes. The pig was assessed for changes in fat reduction over 3 months with digital photography and ultrasound. After euthanasia, tissue sections were harvested and gross pathology and histology were examined.

Results: V-ECLL and P-ECLL treatments led to visible fat reduction (12.1%–27.7% and 9.4%–40.8%, respectively) and contour changes across several parameters. An increased reduction of the superficial fat layer occurred with increased dosimetry parameters with an average charge transfer of 12.5, 24.3, and 47.5 C transferred for 5 V V-ECLL for 5, 10, and 20 minutes, respectively, and 2.0, 11.5, and 24.0 C for –1.5 V P-ECLL, –2.5 V P-ECLL, –3.5 V P-ECLL for 5 minutes, respectively. These dose-dependent changes were also evidenced by digital photography, gross pathology, ultrasound imaging, and histology.

Conclusions: ECLL results in selective damage and long-lasting changes to the adipose layer in vivo. These changes are dose-dependent, thus allowing for more precise contouring of target areas. P-ECLL has greater efficiency and control of total charge transfer compared to V-ECLL, suggesting that a low-voltage potentiostat treatment can result in fat apoptosis equivalent to a high-voltage DC system.

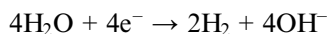
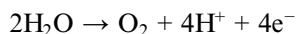
KEYWORDS

body contouring, electrochemical lipolysis, electrochemistry, fat necrosis, fat reduction, fat sculpting, lipolysis, minimally invasive cosmetic procedures

INTRODUCTION

The body fat contouring market is predicted to be valued at \$16.5 billion by 2025.¹ Traditional fat reduction surgeries, including abdominoplasty and liposuction procedures, have been joined by numerous less invasive office-based techniques. Current minimally invasive techniques include hyperthermic laser lipolysis,^{2,3} hyperthermic radiofrequency therapy,⁴ photobiomodulation (PBM),⁵ high-intensity focused ultrasound (HIFU),^{6,7} cryolipolysis,⁸ and the injection of lipolytic drugs (e.g., deoxycholic acid—a bile acid).⁹ Although these procedures are effective at reducing body fat, they can be expensive and may not facilitate selective contouring and reduction of localized areas of fat. This underscores the need for an inexpensive, simple, and minimally invasive means of fat reduction and body contouring. As we have previously demonstrated, electrochemical lipolysis (ECLL) has the potential to be a novel and effective approach to selectively reducing body fat.^{10–12}

ECLL creates localized pH gradients through the formation of hydrogen ions at the anode and hydroxide ions at the cathode. This is achieved through water electrolysis via the reactions:



which occur at the anode and cathode, respectively. Electrochemical therapy (ECT) has been studied in a number of tissues and has been shown to create a localized tissue injury resulting in lengthening of tendons, cartilage reshaping, and collagen remodeling in skin.^{10,13–35} A previous ECT study on fat demonstrated that ECLL results in pH gradients that lead to adipocyte cell deaths via membrane lysis, saponification of triglycerides, and nucleic acid and protein degradation.¹⁰

Our group has demonstrated that ECLL can be accomplished with either a simple open-loop voltage-driven system (V-ECLL) or a potential-driven feedback system (P-ECLL).¹¹ While V-ECLL is simple direct current (DC) system requiring only two electrodes, P-ECLL is based on the use of a potentiostat that incorporates the use of three electrodes: a working, counter, and reference electrode connected by an operational amplifier.³⁶ The reference electrode provides feedback control that allows for sufficient voltage at the counter electrode that sustains a designated potential at the working electrode.³⁶ Our previous ECLL investigations used extremely short needle electrodes (1 cm) inserted perpendicularly to the skin surface to obtain a

tissue response analogous to a point spread function.^{10,11} In this study, a more clinically relevant device was used, which incorporated the insertion of long needle electrodes parallel to the surface of the skin in the subcutaneous fat layer. This produced a trough-like depression in the skin weeks after therapy that is readily observed clinically. The aim of this study is to determine the effects of V-ECLL and P-ECLL targeted fat reduction with a long needle electrode system in an in vivo Yucatan pig model over the course of 3 months. The Yucatan pig is an established clinical model for studying metabolic disorders and fat contouring devices due to its sizable subcutaneous fat layer compared to other domestic pig models such as the Yorkshire or Landrace.^{37,38} The effect of each treatment was evaluated with digital photography, gross pathology, ultrasound, and histology.

MATERIALS AND METHODS**Animal care and anesthesia**

The study was approved by the Institutional Animal Care and Use Committee of the University of California, Irvine (IACUC # AUP-17-164). A 5-year-old, 94 kg female Yucatan pig was housed in the animal facility for 7 days before the start date of the study to allow for acclimation of the pig. The pig was weighed biweekly with minimal fluctuation in weight throughout the study. The animal fasted for 1 day before the initial procedure date. On the procedure date (Day 0), the pig underwent general anesthesia with intramuscular injections of telazol (10 mg/kg) and xylazine (5 mg/kg) and was orally intubated. Anesthesia was maintained with continuous isoflurane gas (1%–3%). Maintenance fluids were administered via Lactated Ringer's solution at a rate of 4 ml/kg/h. Intramuscular enrofloxacin (7.5 mg/kg) was given as antibiotic prophylaxis. Postoperatively, the pig was monitored for pain, distress, infection, bleeding, and other side effects. After 2 months (Day 60) post-treatment, the pig underwent general anesthesia per above protocol for digital photography and ultrasound evaluation. At 3 months (Day 90) after treatment, pentobarbital sodium/phenytoin sodium (0.3 ml/kg) was administered for euthanasia and samples were collected for analysis.

Electrochemical lipolysis

On Day 0, the dorsal side of the animal was first shaved and cleaned with 70% ethanol. The treatment sites were

demarcated on the dorsum of the animal with skin markers (Figure 1). At each treatment site, 60 ml of 0.9% normal saline was injected into the subcutaneous fat along the trajectory of planned needle insertion. Preliminary ex vivo experiments (not included) showed that this volume sufficiently tumesced the adipose tissue to allow for easier needle electrode placement while increasing water content in the fat. The treatment sites were run at least 6 cm away from other treatment sites to ensure that the treated sites would not have an effect on one another. The needle electrodes were created from 80:20 platinum-iridium wires with a 0.813 mm (20 gauge) diameter. The wires were approximately 15 cm and gently curved to assist with the parallel insertion of needles along an 8 cm length in the subcutaneous fat. The needle electrodes exited the skin at both ends and were placed approximately 5 mm apart from each other.

V-ECLL treatments were conducted using a DC power supply at 5 V for 5, 10, and 20 minutes. For these treatments, the anode lead was placed superiorly while the cathode was placed inferiorly (Figures 1A and 2A). To prevent increased electrical resistance due to H₂ and O₂ gas product formation, every 2 minutes the power was turned off for 5 seconds (off-time). During this “off-time,” the porcine skin was massaged to clear gas bubbles from the subcutaneous layer. P-ECLL treatments were conducted similarly but utilized a potentiostat (Model 650, CH Instruments) at the following

parameters: -1.5 , -2.5 , and -3.5 V for 5 minutes. During P-ECLL treatments, no “off-time” was performed as the potentiostat provides a constant potential at the working electrode via feedback from the reference electrode.³⁶ During P-ECLL treatments, the reference needle was placed in the middle, with the counter electrode (anode) placed superiorly and the working electrode (cathode) placed inferiorly (Figures 1B and 2B). All three electrodes were oriented parallel to each other, 5 mm apart. Potentiostat treatments were performed as bulk hydrolysis at a fixed voltage. Each parameter for both V-ECLL and P-ECLL was performed twice at separate treatment sites. To serve as an untreated control (sham), one treatment site was tumesced and three needles were placed but remained disconnected from any power source. Charge transfer data was collected throughout the duration of all ECLL treatments for analysis. Following these treatments, the electrode insertion and exit sites were tattooed with black ink for future identification and tracking. The sites were dressed with gauze and tape and were removed 1 week later.

Assessment

Digital photographs with a DSLR camera (EOS Rebel XS, Canon) and diagnostic portable ultrasound (iQ+, Butterfly) were used to evaluate the target sites, and were

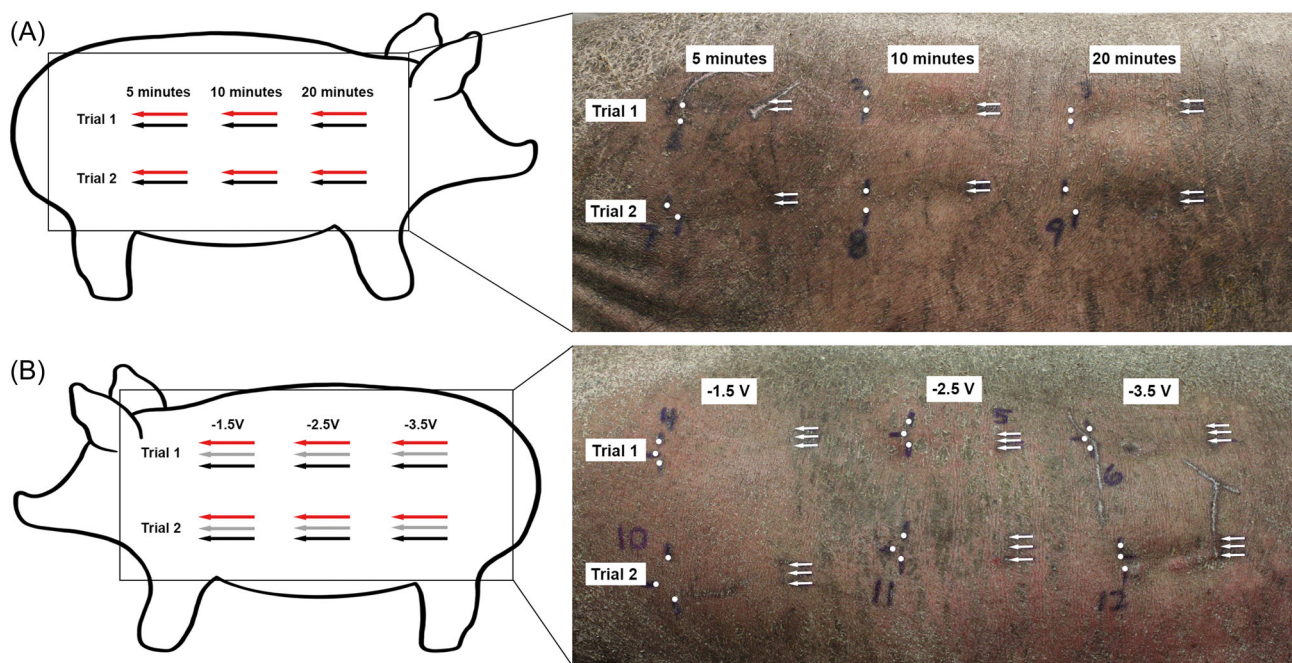


FIGURE 1 (A) V-ECLL treatment layout and photograph of the V-ECLL treatment sites showing skin surface contour changes at the 10-minute and 20-minute sites 3 months after treatment. Red arrows indicate anode placement while black arrows indicate cathode placement. White arrows represent point of needle entry into the skin while white circles indicate the point of needle exit. (B) P-ECLL treatment layout and photograph of the P-ECLL treatment sites showing skin surface contour changes at the -2.5 and -3.5 V sites 3 months after treatment. Red arrows indicate counter electrode placement, gray arrows indicate reference electrode placement, and black arrows indicate working electrode placement. White arrows represent point of needle entry into the skin while white circles indicate the point of needle exit.

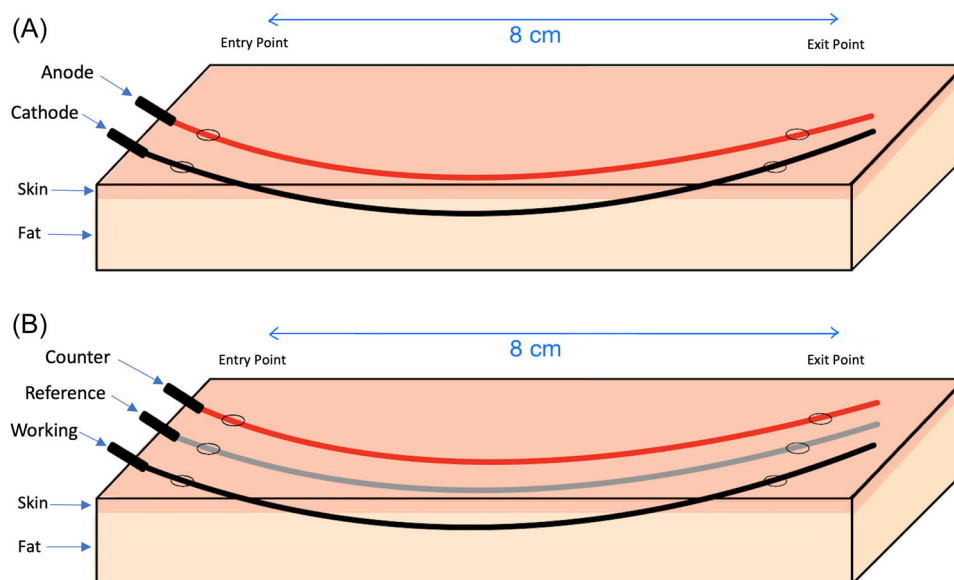


FIGURE 2 (A) Two-needle V-ECLL experimental setup. (B) Three-needle P-ECLL experimental setup.

repeated biweekly. At the 2-month and 3-month time points, the pig was placed under general anesthesia as previously described for thorough physical evaluation of treatment sites with ultrasound and digital photographs. After euthanasia, the treatment sites were sectioned in situ transversely along the treatment axis and were photographed for analysis.

Collected tissue was placed in 10% buffered formalin and processed using standard histologic evaluation.³⁹ The specimens were sectioned 8 μm thick, stained with H&E and α -SMA antibody stains and were evaluated microscopically at 20 \times magnification using a light microscope (BH-2, Olympus).

RESULTS

Digital photography and visual assessment

At the 3-month experimental endpoint, visual evaluation of the pig revealed obvious contour changes (soft tissue depression) at multiple treatment sites. For the V-ECLL treatments, noticeable depressions were evident at 5 V–10 minutes and 5 V–20 minutes treatment sites (Figure 1A). Between these two V-ECLL treatment parameters, the 20-minute treatment sites exhibited greater contouring effect (depression) than the 10-minute treatment sites. With respect to the P-ECLL treatment sites, both the –2.5 V to 5 minutes and –3.5 V to 5 minutes treatment sites exhibited visible contour changes with the –3.5 V to 5 minutes showing a greater effect (Figure 1B). Treatments at –2.5 V to 5 minutes and –3.5 V to 5 minutes P-ECLL sites were wider than that of the V-ECLL which led them to be less noticeable depressions on digital photography. The –3.5 V to 5 minutes P-ECLL

treatment sites showed evidence of probable scar formation, as depicted by the raised and firm areas along the treatment site. This dosed response of increased contour with increased charge transfer for each respective ECLL modality was consistent with gross pathology and ultrasound findings. Subtle hyperpigmented regions at needle entry and exit points of the P-ECLL and V-ECLL treatment sites were present. As expected, the sham site showed no changes in skin pigmentation, contour, or geometry.

Gross pathology and ultrasound evaluation

Gross pathology showed a greater percentage decrease in the thickness of the superficial fat layer at greater dosimetry for both V-ECLL and P-ECLL treatment sites (Table 1). Compared to the sham site, there were color, thickness, and texture changes in the superficial fat layer at each treatment dosimetry consistent with fibrosis (Figure 3). Reduction in the superficial fat layer thickness was more focal with the V-ECLL treatments compared to the P-ECLL treatments; the latter showed a broader contour effect which may be a result of the three-needle array. This finding correlated with the ultrasound images.

The ultrasound examination also demonstrated an increasing reduction of the superficial fat layer as both time for the V-ECLL treatments and voltage for the P-ECLL treatments were increased (Figure 4). These findings were consistent with visual assessment and gross pathology. Hyperechoic areas in the superficial fat layer were noticeable on ultrasound for all ECLL treatment sites and ran longitudinally along the sites. These regions corresponded to the regions of color, thickness, and

texture changes noticed with the gross pathology. No changes were seen at the sham site.

Histology

The sham site showed homogenous adipocytes with regular, circular cell morphology separated by connective tissue and fibroblasts with eccentric nuclei (Figure 5A). V-ECLL and P-ECLL specimens show a visible decrease in the number of adipocytes and a loss of homogeneity in the shape of the adipocytes, suggesting lipid depletion and destruction of adipocytes (Figure 5). There was also

an observed increase in weakly positive α -SMA antibody staining indicative of an increase of myofibroblasts in the treated tissue compared to the sham (Figure 6). The amount of α -SMA antibody stain increased around adipocytes and in vascular vessel lumen as the dosimetry for both V-ECLL and P-ECLL. This increase in myofibroblasts results in the deposition of collagen at the treated sites visualized in Figure 5 of the ECLL-treated sites. The longer the treatment for V-ECLL and the higher the dosimetry for P-ECLL, the more pronounced fibrosis became. At the higher treatment sites (Figure 5D,H), there was a substantial collagen deposition between adipocytes.

TABLE 1 Percent decrease of the superficial fat layer by treatment and trial as seen with gross pathology

Treatment	Trial	Superficial fat layer decrease (%)	
V-ECLL	5 V–5 minutes	1	19.4
		2	12.1
	5 V–10 minutes	1	15.8
		2	23.7
	5 V–20 minutes	1	24.8
		2	27.7
P-ECLL	–1.5 V to 5 minutes	1	11.8
		2	9.4
	–2.5 V to 5 minutes	1	31.9
		2	28.1
	–3.5 V to 5 minutes	1	40.8
		2	28.3

Charge and current transfer data

Current and total charge transfer was recorded as a function of time at a constant of 5 V for V-ECLL (Figure 7A) and at a constant of 5 minutes for P-ECLL (Figure 7B). Total charge transferred was calculated via the integration of current and plotted as a running sum in Figure 7. For the V-ECLL parameters, there was an expected increase in charge transfer with increase in treatment time; this trend is seen in the charge transfer data (Figure 7A). For Trials 1 and 2 of the 5 V–5 minutes V-ECLL parameters, there was a charge transfer of 12.6 and 12.4 Coulombs (C), respectively. Likewise, there was a similar amount of charge transfer between Trials 1 and 2 of the 5 V–10 minutes treatment trials with 22.5 and 26.0 C transferred, respectively. However, there was greater charge transfer for Trial 1 of the 5 V–20 minutes treatment compared to that of Trial 2; approximately 56.3 C versus 38.7 C transferred, respectively. This was due to a brief jump in current likely caused by a brief short circuit of the electrodes during the treatment and

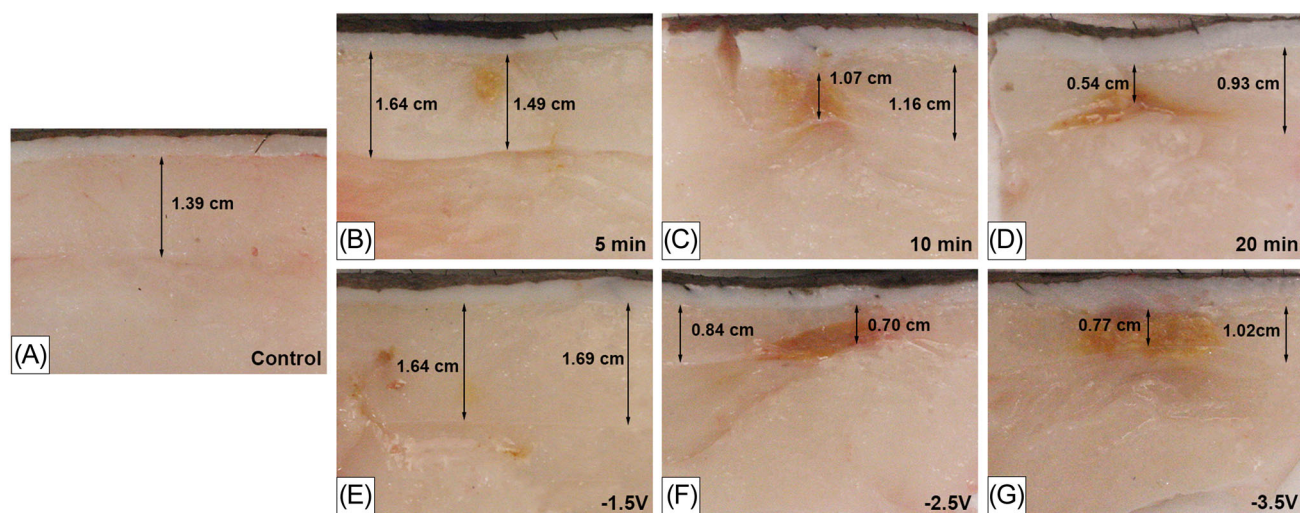


FIGURE 3 Representative gross pathology sections showing (A) control (sham) sites, (B–D) V-ECLL dosimetry treatment sites, and (E–G) P-ECLL dosimetry treatment sites

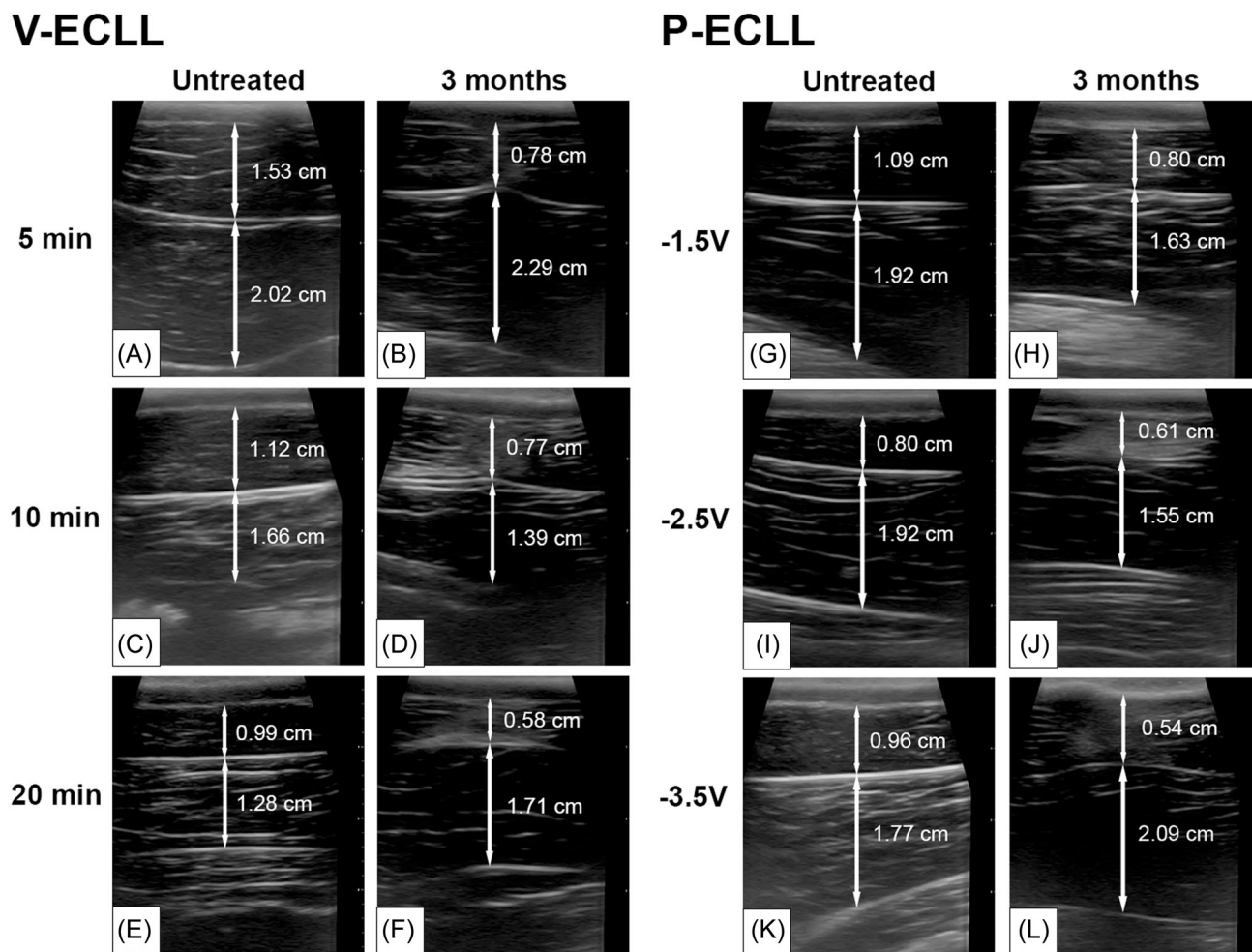


FIGURE 4 Representative ultrasound images of adipose tissue at (A–F) V-ECLL treatment sites when untreated and at the 3-month endpoint and at (G–L) P-ECLL treatment sites when untreated at the 3-month endpoint.

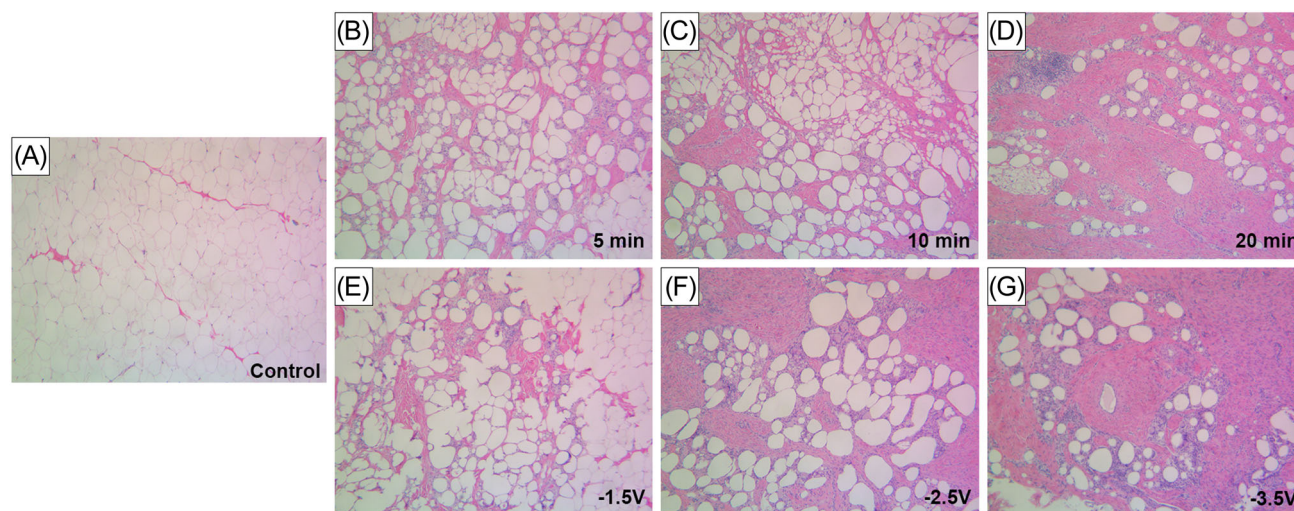


FIGURE 5 Histology of the V-ECLL and P-ECLL-treated regions at 3 months. H&E stained histological images of (A) untreated control (sham), (B–D) V-ECLL treatment sites, and (E–G) P-ECLL treatment sites.

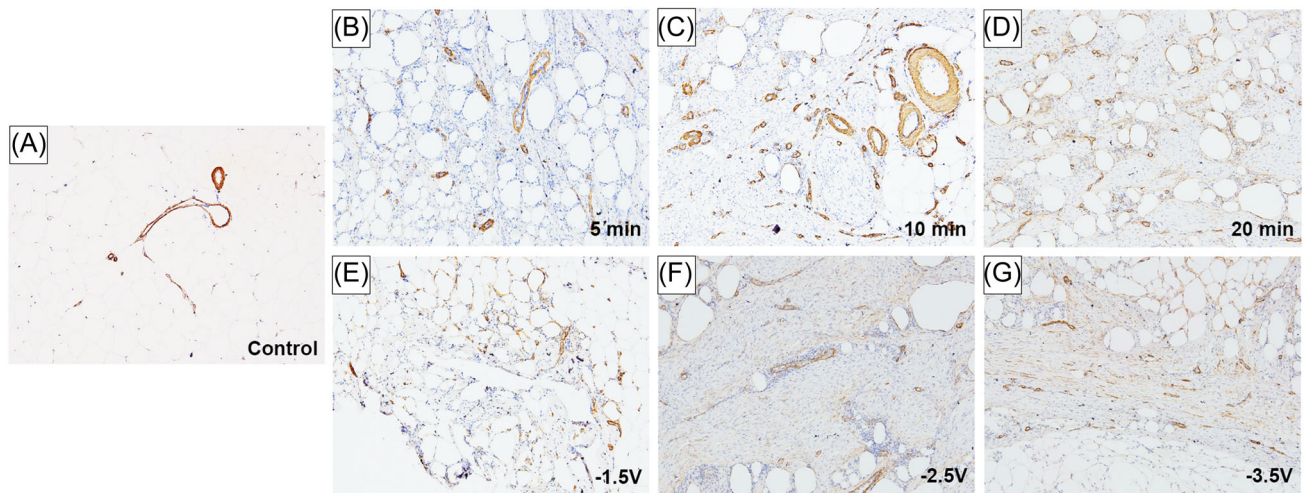


FIGURE 6 Histology of the V-ECLL and P-ECLL-treated regions at 3 months. Alpha-smooth muscle actin stain at the (A) untreated control (sham), (B–D) V-ECLL treatment sites, and (E–G) P-ECLL treatment sites.

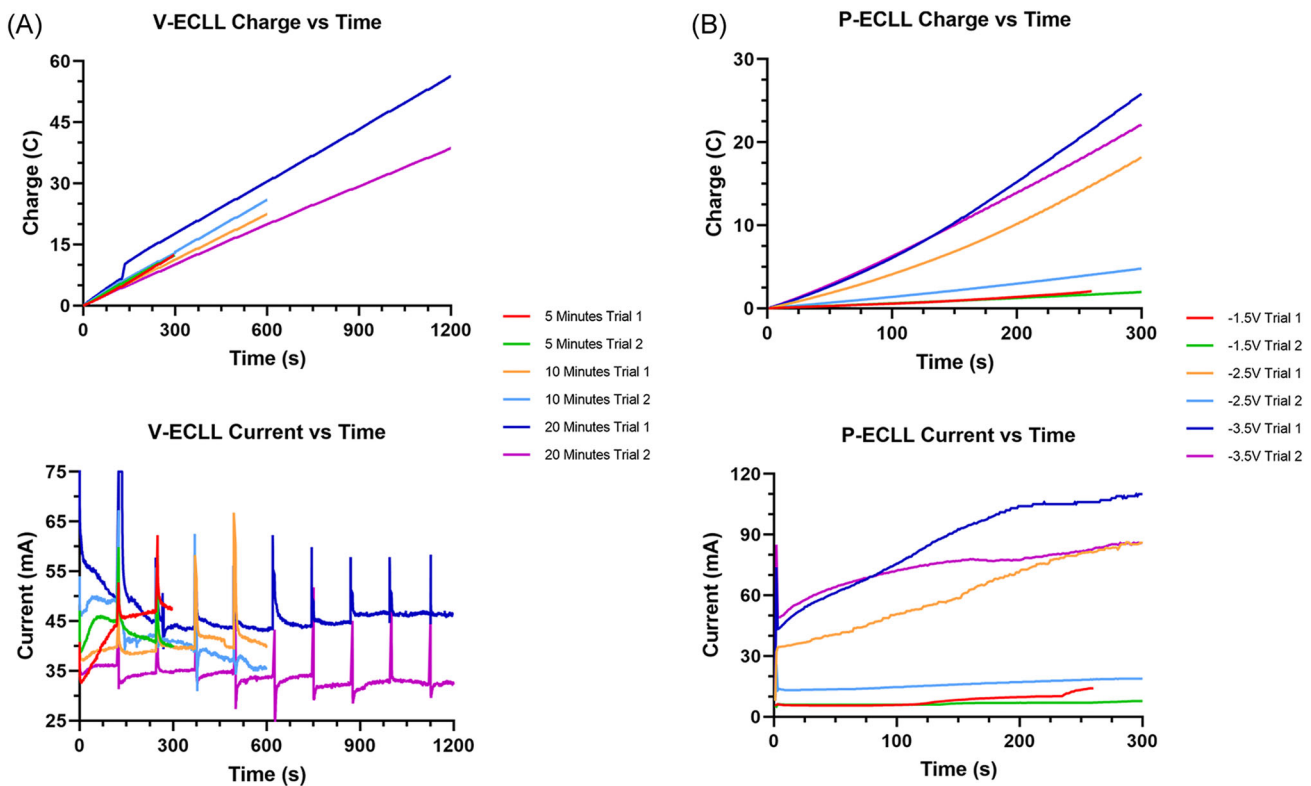


FIGURE 7 (A) In vivo V-ECLL charge vs time and current vs time graphs for V-ECLL dosimetry parameters. (B) In vivo P-ECLL charge vs time and current versus time graphs for P-ECLL dosimetry parameters.

subsequently, an increase in charge transfer at approximately 150-second mark. Current range and variation during V-ECLL treatment was within the expected range (30–50 mA). During each V-ECLL procedure, the 5-second “off-time” at every 2-minute interval and subsequent resumption of the reaction, corresponded to the current spikes observed. This intermittent massage to dissipate the gas bubbles improves the efficiency of the

electrochemistry as gas bubble build-up at the electrodes can lead to increased resistance.

For the P-ECLL parameters, an expected increase in charge transfer was observed with increasing applied potential (Figure 7B). Similarly, there was a marked increase in current as potential increased. For Trials 1 and 2 of the -1.5 V to 5 minutes P-ECLL parameters, there was a charge transfer of 2.04 and 1.96 C,

respectively. Likewise, there was a similar amount of charge transfer between Trials 1 and 2 of the -3.5 V to 5 minutes P-ECLL treatment trials with 25.8 and 22.1 C transferred, respectively. However, there was a substantial difference between Trials 1 and 2 of the -2.5 V P-ECLL treatments with Trial 1 transferring 18.2 C and Trial 2 transferring 4.8 C. The low charge transfer of Trial 2 may have occurred due to differences in the local environments of the reaction which may have been caused by variations in saline distribution or differences in the diffusion of gas formed at the electrodes across the trials.

DISCUSSION

Existing methods for fat reduction range from surgical procedures to less invasive means such as hyperthermic laser lipolysis, hyperthermic radiofrequency therapy, PBM, HIFU, cryolipolysis, and deoxycholic acid. Our group has conducted previous studies showing the feasibility of ECLL as a potential fat contouring and reduction method for cosmetic or medical purposes.^{10–12} Prior *ex vivo* and limited *in vivo* studies have shown that ECLL can induce cell death via membrane lysis, saponification of triglycerides, and nucleic acid and protein degradation.^{10–12} In this longitudinal *in vivo* study, we show that ECLL, both V-ECLL and P-ECLL, lead to sustained adipose tissue contour and reduction in a live Yucatan pig model. The Yucatan pig model was utilized as it is a well-established clinical animal model for studying metabolic disorders and body contouring effects due to its thick subcutaneous fat layer compared to conventional domestic breeds such as the Landrace or Yorkshire.^{37,38} We also demonstrate that P-ECLL can achieve a more dramatic change in contour than V-ECLL.

At the -3.5 V to 5 minutes P-ECLL sites, there was palpable indurated tissue along the needle insertion path which may be consistent with scar tissue formation. This was the highest dosimetry parameter tested for P-ECLL and may represent an upper limit dosimetry limit. Hyperpigmentation of the skin at the needle insertion and exit points was also observed here as in previous studies.^{31,34,35} This is a common effect observed in many energy-based skin therapies and is an unpredictable process associated with moderate tissue injury.^{40–43} This needs to be further explored if this technology is to be directed for treating skin. For a clinical device, simply insulating the needle at its interface with the skin should eliminate this effect.

With ECT, charge transfer determines the amount of acid or base formed, which in turn is proportional to the tissue effect.^{10,12,31,33,35} The degree of charge transfer is controlled by changing electrochemical systems, voltage, and time parameters. Increasing voltage or time parameters results in increasing charge transfer. However, there

was variability of the charge transfer, particularly between Trials 1 and 2 for -2.5 V to 5 minutes P-ECLL likely due to the variation in tissue tumescence. One of the limitations of this method is that a truly homogenous tissue tumescence may be difficult to achieve in a target tissue area. This leads to the local variations of the dosage effect and thus variable outcomes at different treatment sites. In humans, more consistent tumescence may potentially be achieved as the skin is substantially thinner and fat less constrained by connective tissue as in porcine subjects. Another confounding factor includes the bubble formation around electrodes that can lead to transitory increase in local resistance. Our current research effort is focused on reducing and controlling these confounding factors.

Different advantages and limitations exist for each electrochemical system. V-ECLL is a far simpler and cost-effective method that requires only needle electrodes and a simple DC power source (i.e., battery). These components can be purchased at prices as low as \sim $\$5$. However, this method results in the open loop consumption of the electrolytic solution (saline) surrounding the electrodes, leading to potentially longer treatment times as diffusion of water back into the treatment zone is time dependent. This limitation of V-ECLL is addressed in a P-ECLL system that relies on feedback (closed-loop) of a pre-defined local potential and dynamic control of current. P-ECLL provides more control over the electrochemistry by creating a more efficient reagent diffusion-limited system.

The P-ECLL system is the more electrochemically efficient modality that can achieve similar results as V-ECLL but with less time and voltage. Trial 1 of the -2.5 V P-ECLL treatment had a lower charge transfer than that of the 5 V–10 minutes V-ECLL treatments (Figure 7). However, reduction of the superficial fat layer and the extent of fibrosis indicated by gross pathology was equivalent between the two ECLL modalities (Figure 3C,F); this similar tissue effect was further supported by ultrasound data (Figure 4C,D,I,J). Similarly, the two treatments qualitatively exhibited similar histologic fibrosis and adipocyte reduction (Figures 5C,F). While the tissue effects of Trial 1 of the -2.5 V to 5 minutes P-ECLL and 5 V–10 minutes V-ECLL treatments were very similar, the P-ECLL system was able to accomplish this with less time and less total charge transferred, highlighting the increased efficiency and effectiveness of the potentiostat system.

Although changes to the visible contour were more apparent with the naked eye, preliminary results from digital photographs indicate that ECLL results in sustained changes in the adipose layer. Depressions in the subcutaneous tissue layers were observed at the 5 V–10 minutes, 5 V–20 minutes V-ECLL treatment sites, and at the -2.5 V to 5 minutes, -3.5 V to 5 minutes P-ECLL treatment sites. The -2.5 V to 5 minutes P-ECLL site showed visible contour change that appeared less

dramatic than that of the 5 V–10 minutes and 5 V–20 minutes V-ECLL treatments as shown in Figure 1. However, it should be acknowledged that contour change at the –2.5 V P-ECLL site affected a greater surface area, making it appear less noticeable with digital photography. This is due to the three-needle system of the P-ECLL which orients the working electrode and the counter electrode approximately 10 mm from each other while the V-ECLL two-needle system orients the anode and cathode 5 mm from each other. Thus, the different geometry of the electric fields between the two systems may have contributed to the differences in the width of the resulting contours. Further studies should be conducted to investigate the effects of electrode geometry on the spatial treatment on adipose tissue along with local vascular and nervous tissue. Modeling the electrical field is a complex process because the dielectric properties of the tissue change with pH and the ionic composition, and all these variables change during ECT. It is possible to estimate the electric field at the onset of treatment though. The –2.5 V to 5 minutes P-ECLL and 5 V–10 minutes, 5 V–20 minutes V-ECLL treatments produced desirable visible contour changes on the Yucatan pig without the presence of obvious fibrosis upon visual inspection and digital photography. Although this dosimetry may be suitable for this animal model, lower dosage should be explored for future human studies to account for the differences in chemical and mechanical properties of human fat compared to that of Yucatan pigs. Further animal studies should be conducted to further explore ECLL dosimetry that optimizes fat reduction while minimizing fibrosis.

Superficial fat reduction at the treatment sites was correlated with gross pathology and ultrasound. Gross pathology and ultrasound not only exhibited a decrease in the superficial fat layer at the treatment sites that showed visual contour changes, but also showed a decrease in the superficial layer of fat for the 5 V–5 minutes V-ECLL and –1.5 V to 5 minutes P-ECLL treatments. This indicates that even at these lower treatments, there was a local tissue effect that led to fat destruction but did not lead to sufficient volume loss for visible contouring effect. However, fat loss observed with gross pathology is acquired *ex vivo* and is not directly relevant to the clinically desired outcome of visible fat contour.

The visualized contour changes and reduction in the thickness of the fat layer seen with gross pathology and ultrasound also correlate with the histological changes. Histology of the subcutaneous tissue at the sham site demonstrated round adipocytes with regular morphology and distribution. This contrasts with the treated tissue which shows remodeling with an increase in myofibroblasts evidenced by the α -SMA antibody stain. The observed increase in α -SMA antibody stain in the vascular vessel lumen suggests that like other fat contour technology, named vessels should be avoided by clinicians. Compared to the sham site, the treatment sites had

increased fibrosis and collagen deposition. These histological results are comparable to other minimally invasive fat reduction procedures.^{37,44} This fibrosis paired with an evident decrease in adipocytes in treated histology provides evidence of adipocyte destruction due to cell membrane lysis, nuclear degradation, and triglyceride saponification which increased the proportion of collagen in the tissue as observed in previous studies.^{10–12,38,44} A previous study by our group utilized a live-dead assay to show the viability of the remaining adipocytes after ECLL treatment; however, the metabolic function of these adipocytes should be investigated in future studies.¹⁰ The higher the dosimetry parameters, the greater the proportion of observed collagen and the less the proportion of remaining adipocytes following treatment. Scar formation is likely dose-dependent as demonstrated in this study with the broad range of electrochemical device parameters. The formation of scar for specific tissue contouring may actually be useful in other clinical applications such as contouring around the abdominal musculature (six-pack abs). On the other hand, longer survival studies in this animal model may potentially show further remodeling and potential disappearance of this scar tissue beyond 3 months. In this proof of concept study, extreme dosimetries resulting in fibrosis were selected to clearly visualize the macroscopic effects of the treatment. Further studies should be conducted to explore more clinically relevant dosimetries and to observe tissue effects beyond 3 months.

This pilot study, while limited in one subject, demonstrates the efficacy of this technology in an animal model where a sizable and suitable subcutaneous fat layer exists. This validates the potential use of two modes of ECLL as they can achieve desirable changes in the adipose tissue of a longitudinal *in vivo* animal study. Future work would aim to develop parameters that would be optimized for human subjects.

CONCLUSION

ECLL of adipose tissue results in spatially localized damage in the adipose tissue thus allowing for dose-dependent targeted fat treatment. Both V-ECLL and P-ECLL treatments at higher dosimetry were shown to decrease the thickness of the superficial fat layer; however, P-ECLL was able to do so in a more efficient manner than V-ECLL. This reduction in fat is evident in the digital photography, ultrasound, gross pathology, and histology of this study.

ACKNOWLEDGMENTS

This research received financial support from The Nicholas Endowment Grant, UCI Beall Applied Innovation, and the Leading Foreign Research Institute Recruitment Program through the National Research Foundation of Korea (NRF) funded by the Ministry of Science and ICT (MSIT) (NRF-2018K1A4A3A02060572).

CONFLICT OF INTEREST

The authors declare no conflict of interest.

ORCID

Asher C. Park  <http://orcid.org/0000-0002-3631-463X>
 Ellen M. Hong  <http://orcid.org/0000-0002-0084-2924>
 Brian J. F. Wong  <https://orcid.org/0000-0001-6318-7384>

REFERENCES

- Body Fat Reduction Market Size By Procedure (Surgical {Liposuction, Abdominoplasty}, Non-surgical {Cryolipolysis, Ultrasound, Laser Lipolysis}), By Gender Sumant Ugalmugale RS (Female, Male), By Service Provider (Hospitals, Clinics, Medical Spas), Industry Analysis Report, Regional Outlook, Application Potential, Price Trends, Competitive Market Share & Forecast, 2020–2026. Accessed 15 Dec 2021. https://www.gminsights.com/industry-analysis/body-fat-reduction-market?utm_source=prnewswire.com%26amp;utm_medium=referral%26amp;utm_campaign=Paid_prnewswire
- McBean JC, Katz BE. Laser lipolysis: an update. *J Clin Aesthet Dermatol.* 2011;4(7):25–34.
- Milanic M, Muc BT, Jezersek M, Lukac M. Experimental and numerical assessment of hyperthermic laser lipolysis with 1,064 nm Nd:YAG laser on a porcine fatty tissue model. *Lasers Surg Med.* 2018;50(2):125–36. <https://doi.org/10.1002/lsm.22743>
- Franco W, Kothare A, Ronan SJ, Grekin RC, McCalmont TH. Hyperthermic injury to adipocyte cells by selective heating of subcutaneous fat with a novel radiofrequency device: feasibility studies. *Lasers Surg Med.* 2010;42(5):361–70. <https://doi.org/10.1002/lsm.20925>
- Shanks S, Leisman G. Perspective on broad-acting clinical physiological effects of photobiomodulation. *Adv Exp Med Biol.* 2018;1096:41–52. https://doi.org/10.1007/5584_2018_188
- Saedi N, Kaminer M. New waves for fat reduction: high-intensity focused ultrasound. *Semin Cutan Med Surg.* 2013;32(1):26–30.
- Palumbo P, Cinque B, Miconi G, La Torre C, Zoccali G, Vrentzos N, Vitale AR, Leocata P, Lombardi D, Lorenzo C, D'Angelo B, Macchiarelli G, Cimini A, Cifone MG, Giuliani M. Biological effects of low frequency high intensity ultrasound application on ex vivo human adipose tissue. *Int J Immunopathol Pharmacol.* 2011;24(2):411–22. <https://doi.org/10.1177/039463201102400214>
- Ingargiola MJ, Motakef S, Chung MT, Vasconez HC, Sasaki GH. Cryolipolysis for fat reduction and body contouring: safety and efficacy of current treatment paradigms. *Plast Reconstr Surg.* 2015;135(6):1581–90. <https://doi.org/10.1097/PRS.0000000000001236>
- Ascher B, Fellmann J, Monheit G. ATX-101 (deoxycholic acid injection) for reduction of submental fat. *Expert Rev Clin Pharmacol.* 2016;9(9):1131–1143. <https://doi.org/10.1080/17512433.2016.1215911>
- Pham TT, Stokolosa AM, Borden PA, Hansen KD, Hong EM, Krasieva TB, Sivoraphonh RH, Moy WJ, Heidari AE, Lee LH, Kim EH, Sun CH, Jia W, Mo JH, Kim S, Hill MG, Wong BJF. Electrochemical degradation and saponification of porcine adipose tissue. *Sci Rep.* 2020;10(1):20745. <https://doi.org/10.1038/s41598-020-76678-y>
- Heidari AE, Hong EM, Park A, Pham TT, Steward E, Chen LY, Qu Y, Dunn BS, Seo SH, Patel U, Dilley K, Hakimi AA, Syed A, Kim S, Hill MG, You JS, Wong BJF. Exploring feedback-controlled versus open-circuit electrochemical lipolysis in ex vivo and in vivo porcine fat: a feasibility study. *Lasers Surg Med.* 2021;54:157–69. <https://doi.org/10.1002/lsm.23466>
- Hutchison DM, Hakimi AA, Hong EM, Pham TT, Wijayaweera A, Seo S, Qu Y, Bircan M, Sivoraphonh R, Dunn B, Sun CH, Kobayashi MR, Kim S, Wong BJF. Electrochemolipolysis of human adipose tissue. *Facial Plast Surg Aesthet Med.* 2020;22(2):86–92. <https://doi.org/10.1089/fpsam.2019.29011.hut>
- Ho KHK, Valdes SHD, Protsenko DE, Aguilar G, Wong BJF. Electromechanical reshaping of septal cartilage. *Laryngoscope.* 2003;113(11):1916–21. <https://doi.org/10.1097/00005537-200311000-00011>
- Protsenko DE, Ho K, Wong BJF. Stress relaxation in porcine septal cartilage during electromechanical reshaping: mechanical and electrical responses. *Ann Biomed Eng.* 2006;34(3):455–64. <https://doi.org/10.1007/s10439-005-9051-y>
- Chae Y, Protsenko D, Holden PK, Chlebicki C, Wong BJF. Thermoforming of tracheal cartilage: viability, shape change, and mechanical behavior. *Lasers Surg Med.* 2008;40(8):550–61. <https://doi.org/10.1002/lsm.20666>
- Manuel CT, Foulad A, Protsenko DE, Sepehr A, Wong BJF. Needle electrode-based electromechanical reshaping of cartilage. *Ann Biomed Eng.* 2010;38(11):3389–97. <https://doi.org/10.1007/s10439-010-0088-1>
- Manuel CT, Foulad A, Protsenko DE, Hamamoto A, Wong BJF. Electromechanical reshaping of costal cartilage grafts: a new surgical treatment modality. *Laryngoscope.* 2011;121(9):1839–42. <https://doi.org/10.1002/lary.21892>
- Wu EC, Protsenko DE, Khan AZ, Dubin S, Karimi K, Wong BJF. Needle electrode-based electromechanical reshaping of rabbit septal cartilage: a systematic evaluation. *IEEE Trans Biomed Eng.* 2011;58(8):2378–83. <https://doi.org/10.1109/TBME.2011.2157155>
- Lim A, Protsenko DE, Wong BJF. Changes in the tangent modulus of rabbit septal and auricular cartilage following electromechanical reshaping. *J Biomech Eng.* 2011;133(9):094502. <https://doi.org/10.1115/1.4004916>
- Protsenko DE, Ho K, Wong BJF. Survival of chondrocytes in rabbit septal cartilage after electromechanical reshaping. *Ann Biomed Eng.* 2011;39(1):66–74. <https://doi.org/10.1007/s10439-010-0139-7>
- Badran K, Manuel C, Waki C, Protsenko D, Wong BJF. Ex vivo electromechanical reshaping of costal cartilage in the New Zealand white rabbit model. *Laryngoscope.* 2013;123(5):1143–8. <https://doi.org/10.1002/lary.23730>
- Oliaei S, Manuel C, Karam B, Hussain SF, Hamamoto A, Protsenko DE, Wong BJF. In vivo electromechanical reshaping of ear cartilage in a rabbit model: a minimally invasive approach for otoplasty. *JAMA Facial Plast Surg.* 2013;15(1):34–8. <https://doi.org/10.1001/2013.jamafacial.2>
- Tracy LE, Wong BJ. The effect of pH on rabbit septal cartilage shape change: exploring the mechanism of electromechanical tissue reshaping. *Eplasty.* 2014;14:23.
- Yau AYY, Manuel C, Hussain SF, Protsenko DE, Wong BJF. In vivo needle-based electromechanical reshaping of pinnae: New Zealand White rabbit model. *JAMA Facial Plast Surg.* 2014;16(4):245–52. <https://doi.org/10.1001/jamafacial.2014.85>
- Badran KW, Manuel CT, Loy AC, Conderman C, Yau YY, Lin J, Tjoa T, Su E, Protsenko D, Wong BJF. Long-term in vivo electromechanical reshaping for auricular reconstruction in the New Zealand white rabbit model. *Laryngoscope.* 2015;125(9):2058–66. <https://doi.org/10.1002/lary.25237>
- Hussain S, Manuel CT, Protsenko DE, Wong BJF. Electromechanical reshaping of ex vivo porcine trachea. *Laryngoscope.* 2015;125(7):1628–32. <https://doi.org/10.1002/lary.25189>
- Kim S, Manuel C, Wong B, Chung PS, Mo JH. Handheld-level electromechanical cartilage reshaping device. *Facial Plast Surg.* 2015;31(3):295–300. <https://doi.org/10.1055/s-0035-1555623>
- Manuel CT, Tjoa T, Nguyen T, Su E, Wong BJF. Optimal electromechanical reshaping of the auricular ear and long-term outcomes in an in vivo rabbit model. *JAMA Facial Plast Surg.* 2016;18(4):277–84. <https://doi.org/10.1001/jamafacial.2016.0166>

29. Hunter BM, Kallick J, Kissel J, Herzig M, Manuel C, Protsenko D, Wong BJF, Hill MG. Controlled-potential electrochemical reshaping of cartilage. *Angew Chem Int Ed*. 2016;55(18):5497–500. <https://doi.org/10.1002/anie.201600856>
30. Moy WJ, Su E, Chen JJ, Oh C, Jing JC, Qu Y, He Y, Chen Z, Wong BJF. Association of electrochemical therapy with optical, mechanical, and acoustic impedance properties of porcine skin. *JAMA Facial Plast Surg*. 2017;19(6):502–9. <https://doi.org/10.1001/jamafacial.2017.0341>
31. Pham TT, Hong EM, Moy WJ, Zhao J, Hu AC, Barnes CH, Borden PA, Sivoraphonh R, Krasieva TB, Lee LH, Heidari AE, Kim EH, Nam SH, Jia W, Mo JH, Kim S, Hill MG, Wong BJF. The biophysical effects of localized electrochemical therapy on porcine skin. *J Dermatol Sci*. 2020;97(3):179–86. <https://doi.org/10.1016/j.jdermsci.2020.01.006>
32. Nguyen TD, Hu AC, Protsenko DE, Wong BJF. Effects of electromechanical reshaping on mechanical behavior of ex vivo bovine tendon. *Clin Biomech*. 2020;73:92–100. <https://doi.org/10.1016/j.clinbiomech.2020.01.009>
33. Hu AC, Hong EM, Toubat O, Sivoraphonh R, Barnes C, Moy WJ, Krasieva TB, Wong BJF. Multiphoton microscopy of collagen structure in ex vivo human skin following electrochemical therapy. *Lasers Surg Med*. 2020;52(3):196–206. <https://doi.org/10.1002/lsm.23094>
34. Hong EM, Pham TT, Seo S, Moy WJ, Borden P, Hansen K, Kim S, Mo JH, Wong BJF. Electrochemical therapy of in vivo rabbit cutaneous tissue. *Laryngoscope*. 2021;131(7):E2196–203. <https://doi.org/10.1002/lary.29461>
35. Hutchison DM, Hakimi AA, Wijayaweera A, Seo S, Hong EM, Pham TT, Bircan M, Sivoraphonh R, Dunn B, Kobayashi MR, Kim S, Wong BJ. Electrochemical treatment of ex vivo human abdominal skin and potential use in scar management: a pilot study. *Scars Burns Heal*. 2021;7:2059513120988532. <https://doi.org/10.1177/2059513120988532>
36. Allen J, Bard LRF. Chapter 15: Electrochemical instrumentation. *Electrochemical methods: fundamentals and applications*. 2nd ed. New York: John Wiley & Sons; 2002.
37. Curtasu MV, Knudsen KEB, Callesen H, Purup S, Stagsted J, Hedemann MS. Obesity development in a miniature Yucatan pig model: a multi-compartmental metabolomics study on cloned and normal pigs fed restricted or ad libitum high-energy diets. *J Proteome Res*. 2018;18(1):30–47. <https://doi.org/10.1021/acs.jproteome.8b00264>
38. Zelickson B, Egbert BM, Preciado J, Allison J, Springer K, Rhoades RW, Manstein D. Cryolipolysis for noninvasive fat cell destruction: initial results from a pig model. *Dermatol Surg*. 2009;35(10):1462–70. <https://doi.org/10.1111/j.1524-4725.2009.01259.x>
39. Clarke GM, Eidt S, Sun L, Mawdsley G, Zubovits JT, Yaffe MJ. Whole-specimen histopathology: a method to produce whole-mount breast serial sections for 3-D digital histopathology imaging. *Histopathology*. 2007;50(2):232–42. <https://doi.org/10.1111/j.1365-2559.2006.02561.x>
40. Thi Kim CN, Thi LP, Nguyen Van T, Thi Minh PP, Vu Nguyet M, Le Thi M, Dinh Huu N, Tran Hau K, Gandolfi M, Satolli F, Feliciani C, Vojvodic A, Tirant M, Lotti T. Successful treatment of facial atrophic acne scars by fractional radiofrequency microneedle in Vietnamese patients. *Open Access Maced J Med Sci*. 2019;7(2):192–4. <https://doi.org/10.3889/oamjms.2019.002>
41. Zhang Z, Fei Y, Chen X, Lu W, Chen J. Comparison of a fractional microplasma radio frequency technology and carbon dioxide fractional laser for the treatment of atrophic acne scars: a randomized split-face clinical study. *Dermatol Surg*. 2013;39(4):559–66. <https://doi.org/10.1111/dsu.12103>
42. Chandrashekar B, Sriram R, Mysore R, Bhaskar S, Shetty A. Evaluation of microneedling fractional radiofrequency device for treatment of acne scars. *J Cutan Aesthet Surg*. 2014;7(2):93–7. <https://doi.org/10.4103/0974-2077.138328>
43. Khalili M, Amiri R, Mohammadi S, Iranmanesh B, Aflatoonian M. Efficacy and safety of traditional and surgical treatment modalities in segmental vitiligo: a review article. *J Cosmet Dermatol*. 2022;21(6):2360–73. <https://doi.org/10.1111/jocd.14899>
44. Walker PS, Lee DR, Toth BA, Bowen B. Histological analysis of the effect of ATX-101 (deoxycholic acid injection) on subcutaneous fat: results from a phase I open-label study. *Dermatol Surg*. 2020;46(1):70–7. <https://doi.org/10.1097/DSS.0000000000001851>

How to cite this article: Park AC, Chan CK, Hutchison DM, Patel U, Hong EM, Steward E, et al. In vivo electrochemical lipolysis of fat in a Yucatan pig model: A proof of concept study. *Lasers Surg Med*. 2023;55:135–145. <https://doi.org/10.1002/lsm.23620>